Journal of Engineering Research and Applied Science
Available at www.journaleras.com
Volume 13 (1), June 2024, pp 2476-2482
ISSN 2147-3471 © 2024

Electrochemical Behaviour of Stainless Steel L80 in a Multiphase Environment

Naima Ghemmit-Doulache[1,*], Hamouche Aksas[2], Nacera Ouslimani[1]

[1] Fibrous Polymer Processing and Shaping Laboratory, Search block, independence avenue; M'Hamed Bougara University, Boumerdes-Algeria.
[2] University of M'Hamed Bougara-Boumerdes, Faculty of Technology, Frantz Fanon city, Boumerdes-Algeria.

Accepted 21 February 2024

Abstract
In this study, we focused on a gas field of Gassi Touil-Algeria where different reports showed failures of steel, caused mainly by corrosion and cracking. Thus, this work contributes to inhibition of stainless steel L80 by an amine-based inhibitor N-(2-aminoethyl). Results of this work indicate that for protection of stainless steel L80 immersed in a multiphase medium, N-(2-aminoethyl) amine-based corrosion inhibitor has a satisfactory protective power. In addition, this inhibitor can be widely used, in particular because of its low toxicity towards environment. For a dose of 50 ppm of this inhibitor, inhibiting efficiency obtained by polarization resistance technique is 93%, and that measured by charge transfer resistance of Electrochemical Impedance Spectroscopy (EIS) technique is 99.9%. Inhibitor addition to multiphase medium increased polarization resistance of L80 steel, and slowed down its corrosion rate from 9.95E-3 to 7.11E^{-5} mm/year for 0 to 50 ppm of inhibitor. EIS results clearly show increase in capacitive loop diameter as inhibitor concentration increases, in line with the increase in polarization resistance.

Keywords: *Corrosion inhibition, Chemical composition, OCP, RP, EIS, SEM.*

1. Introduction
Metal equipment in the petroleum industry is generally subject to various forms of corrosion, particularly pipelines. This phenomenon has gained considerable importance nowadays, given the increasing use of metals and alloys in modern life [1-3]. Corrosion is the most common degradation in hydrocarbons production and is the cause of the majority of failures in pipeline pressure equipment [4-6]. Corrosion is responsible for the destruction of a quarter of the world's steel production each year [7-9]. Metal appearance and action mode of the environment determine the types and corrosion forms. This phenomenon manifests itself inside and outside the stainless steels equipment "pipelines". Because of the aqueous solutions of salts that accompany the production of hydrocarbons such as oil, condensate and gases, often loaded with CO_2 and H_2S, which make these media (multiphase media) corrosive to the material with which the production equipment only delays the production work [10, 11]. Namely, the dissolution of CO_2 and H_2S in a liquid medium leads to various corrosion phenomena in steel [12]. In Algeria, for example, the pipeline network, which has been in operation for about 35 years, has been the victim of corrosion phenomena, the problem being that the rate of evolution has exceeded estimates [11]. Stainless steels known for their use in oil production pipelines [12] and in areas where protection against corrosion is important [13]. However, unfortunately, stainless steels are exposed to considerable wear and tear, e.g. scratching, which hampers the wider applicability of the material and can cause problems in existing applications [14]. Therefore, it is necessary to know the phenomenon of corrosion and its processes in order to find the most effective way of prevention. The most commonly used method for protection against internal corrosion of metallic pipes, and the least expensive, is to select a suitable corrosion inhibitor. The latter requires the use of chemical substances which, when added in very small quantities to the aggressive medium, can reduce the corrosion rate of the exposed metal [15]. Inhibitors can affect the reaction either anodically or cathodically, forming a barrier that protects the metal surface from corrosives [16]. This study, we focused on a gas field of Gassi Touil-Algeria where different reports showed failures of the steel, caused mainly by corrosion and cracking. Thus, this work contributes to the inhibition of L80

* Corresponding author: n.ghemmit@univ-boumerdes.dz

stainless steel by an amine-based inhibitor N-(2-aminoethyl) [17].

2. Materials and methods

2.1. Sampling and working electrode preparation

Material studied is a L80 stainless steel, taken from Gassi Touil-Algeria gas field pipelines, shows layers of corrosion products and pitting defects on its internal surface (figure 1). The sample was cut with a metal saw into a square of $1cm^2$. It was then, welded to a conductive wire and embedded in a thermosetting resin (LECOSET 7007) in a plastic mould exposed to ambient air for 24 hours to allow the resin to solidify. Before each manipulation, the working electrode must undergo a polishing of its surface with silicon carbide (SiC) abrasive papers of decreasing granulometry from 100-2000. For the finishing, we used a suspension of alumina Al_2O_3 and the diamond paste dispersed on a felt glued to a rotating disc to obtain a so-called "mirror polished" surface. Before using the electrode, it must be rinsed with distilled water, degreased with acetone and air-dried.

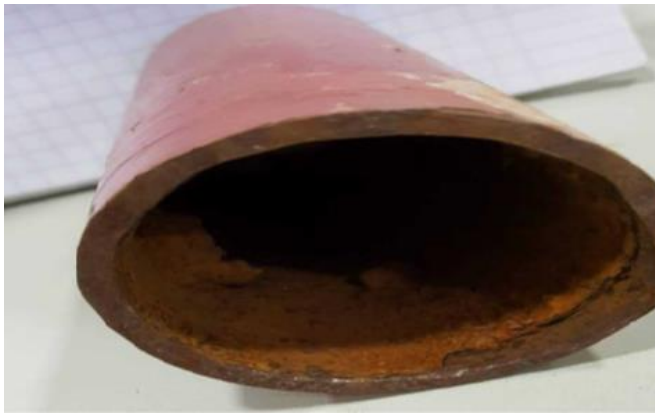

Figure 1: Corroded stainless steel pipeline [13].

2.2. Material chemical composition

The chemical composition of the material was measured spectrophotometrically, using a "PMI-MASTER PRO" spectrophotometer in the laboratory of the Entreprise Nationale de Grands Travaux Pétroliers (ENGTP) in Réghaïa-Algeria.

2.3. Electrolyte

The electrolyte used is a multiphase medium consisting of:

- 560 mL of condensation water: recovered from the pipelines of Gassi-Touil field. This water comes from the production of petroleum by the effect of temperature and pressure. It has a salinity of 2.5g/L NaCl.
- 140 mL of condensate: consisting of a mixture of paraffinic hydrocarbons (saturated hydrocarbons) with molecules containing 5 to 15 carbon atoms. They have characteristics similar to naphtha, generally extracted from the condensate gas fields. It is in liquid form under normal conditions of temperature and pressure [18].
- CO_2 gas.

The medium is desaerated during the test with nitrogen to remove all traces of oxygen.

2.4. Gas corrosion inhibitor

Inhibitor used in this study is an N-(2-aminoethyl) amine-based and used in oil/gas refining and extraction as an anticorrosion agent [19]. The physico-chemical characteristics shown in Table 1.

Table 1. Typical physico-chemical characteristics of gas corrosion inhibitor used.

Appearance	Dark brown liquid
Density at 15 °C	$0.91g/cm^3$
pH (5% aq)	-10.6 ± 0.5
Flash point (°C)	40 °C
Stability limit a cold	-17 °C
Solubility	Aromatic solvent: soluble, - Diesel: Dispersible, - Paraffin: Dispersible, - Water: Dispersible, - Brine (10% NaCl): Dispersible, - Acid (15% HCL): Dispersible.

2.5. Electrochemical cell

The used electrochemical cell consists of three electrodes: a working electrode in stainless steel L80, two counter electrodes in graphite and a reference electrode in saturated calomel ECS. The cell has a 1000 ml volume, is made of Pyrex glass and has a cover with five holes for the fixed positioning of the various electrodes.

Table 2: Chemical composition of L80 stainless steel in % by mass.

Element	Fe	Cr	Ni	Mo	Mn	S	Si	C	Al	Co	Cu
Content (%)	79.98	13.25	5.22	0.76	0.63	0.008	0.14	0.01	0.031	3	0.09

3. Results and discussion

Chemical analysis of stainless steel grade L80 yielded the chemical composition shown in Table 2.

By examining the chemical composition of the sample in Table 2, we find that the content of other elements is above 8%. This explains that our sample is highly alloyed [21, 22]. Similarly, the chromium content is higher than 10.5%, which implies that the sample is a stainless steel (Cr= 13.25) [23, 24]. The contents of chromium (Cr), copper (Cu), manganese (Mn), sulphide (S) and silicium (Si) correspond to standard requirement AP15CT [25]. On the other hand, the contents of carbon (C) and nickel (Ni) are not in conformity.

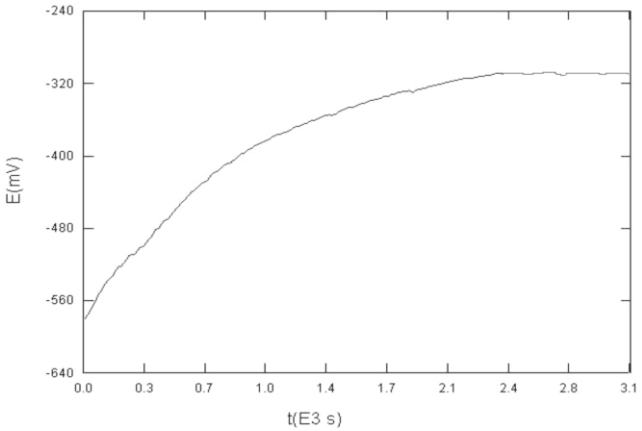

Figure 2: OCP evolution of L80 stainless steel versus time.

The evolution of the free OCP of L80 stainless steel in the multiphase medium (water/condensate in the ratio 80/20) and bubbled by CO_2 gas gave the curves shown in figure 2. The corrosion potential E = Ecorr is measured at zero current (I = 0), it indicates the time needed to reach the equilibrium potential where the rates of the forward and reverse reactions are equal. According to the curve, we note a regular increase of the potential until 2400 seconds when it stabilizes at a value of -320 mV/ECS. This evolution attributed to a dissolution of the stainless steel and its stabilization by formation of a protective film of corrosion product on its surface [26].

Polarization resistance tests of L80 stainless steel in multiphase media in the presence and absence of corrosion inhibitor registered at a potential scan speed of 0.166 mV/SCE, and applying a constant potential around Ecorr ± 10 mV [27]. The electrochemical parameters of polarization resistance results grouped in Table 3 showed us that L80 steel immersed in a multiphase medium without inhibitor exhibits a low Rp of the order of 25.61 KΩ.cm^2. On the other hand, after injection of gas corrosion inhibitor at different concentrations, polarization resistance of the steel increases to 358.4 KΩ.cm^2; which corresponds to a low corrosion rate of order of 10^{-5} mm/year (Figure 3). A protective power of 93% is obtained at 50 ppm corrosion inhibitor (Table 3), calculated according to equation (1) [28].

$$\boldsymbol{E}\ (\%) = \frac{\boldsymbol{RPwith\ inhibitor - RPwithout\ inhibitor}}{\boldsymbol{RPwith\ inhibitor}} \times \mathbf{100} \qquad (1)$$

Table 3: Polarization resistance electrochemical parameters of L80 stainless steel in a multiphase medium in presence and absence of inhibitor.

[Inhibitor] (ppm)	RP (KΩ.cm^2)	Vcorr (mm /an)	Icorr (µA/cm^2)	Ecorr (µA/cm^2)	Efficiency (%)
0	25.61	$9.95.10^{-3}$	0.848	-0.408	_
20	95.43	$2.67.10^{-3}$	0.227	-0.238	73
30	117.5	216.10^{-6}	$18.48.10^{-3}$	-0.232	78
50	358.4	$7.11.10^{-5}$	$60.60.10^{-3}$	-0.238	93

EIS measurements were performed at 10 mV amplitude over a frequency range from 100 kHz to 1 mHz. Nyquist diagrams constructed from measurements taken at different inhibitor concentrations. Impedance diagrams represented in Nyquist and Bode mode (figure 4). Indeed, we recorded two loops; the first one related to activation phenomenon, the diameter of which increases with the concentration of the inhibitor and another loop due to adsorption of the inhibitor on the active sites of the unblocked steel surface. Bode diagrams confirmed this where two-time constants clearly appear, one at high frequency and other at low frequency.

According to equation (2), we can estimate the efficiency of the inhibitor $\boldsymbol{E}$ (%) , calculated from different values of charge transfer resistance (Table 4), where Rct/inh and Rct are the charge transfer resistance with and without inhibitor, respectively [29-31].

$$\boldsymbol{E}\ (\%) = \frac{\boldsymbol{Rct/inh - Rct}}{\boldsymbol{Rct/inh}} \times \mathbf{100} \qquad (2)$$

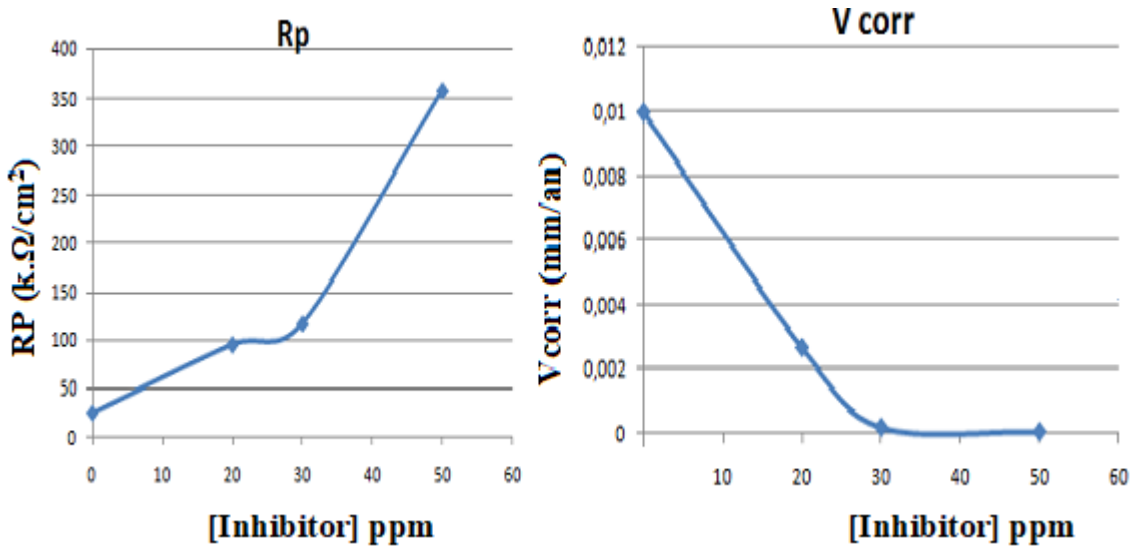

Figure 3: Respective evolution of polarization resistance and corrosion rate of L80 stainless steel for different inhibitor concentrations.

Table 4. EIS electrochemical parameters of L80 stainless steel in a multiphase medium in presence and absence of inhibitor.

[Inhibitor] (ppm)	Rs (KΩ .cm^2)	Rtc (KΩ .cm^2)	Rp (KΩ.cm^2)	Cdl (F/cm^2)	θ	Efficiency (%)
0	0.042	23.166	23.208	0.00032	-61	_
20	0.059	25.345	25.404	0.00037	-75	8.64
30	0.102	1.06.10^6	1060000.102	0.00038	-68	99.9
50	0.132	7.21.10^6	7210000.132	0.00026	-68	99.9

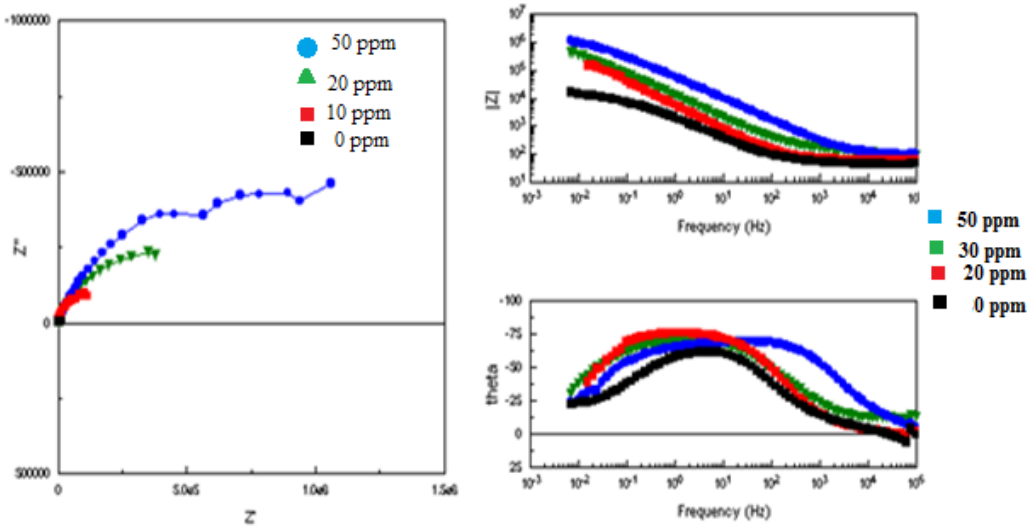

Figure 4. Nyquist and Bode plots of L80 stainless steel electrode without and with inhibitor.

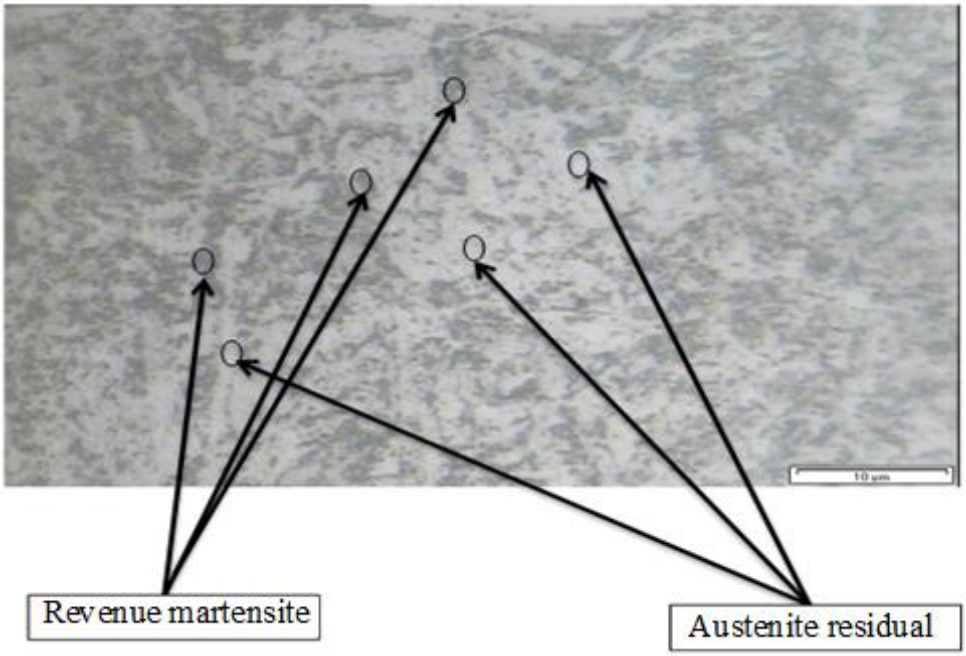

Figure 5. Optical micrograph of L80 stainless steel at 2000x magnification.

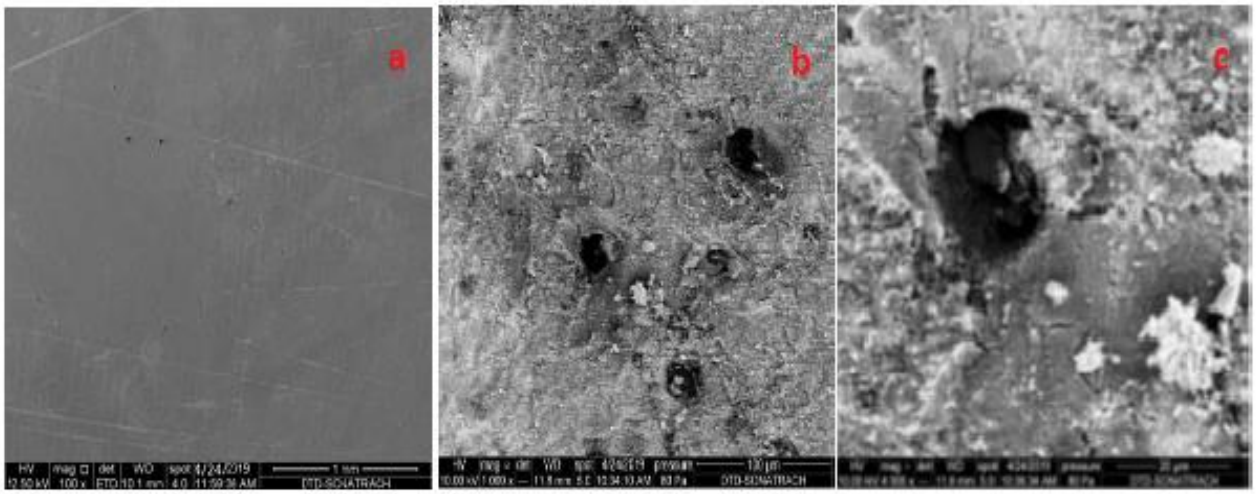

Figure 6. L80 stainless steel SEM images a) without immersion, b), c) after immersion in multiphase medium for 7 days at different magnifications.

Optical microscopic observation of L80 stainless steel surface, chemically attacked by (25% water, 25% HNO_3, 50% HCl), for 3 to 5 seconds, revealed microstructures consisting of martensite and residual austenite (figure 5).

Photo a) of figure 6 shows that surface of L80 steel sample, before its immersion in aggressive medium and inhibitor addition, is clean and does not show any attacked sites. However, photos b) and c) of same figure show appearance of chromium oxide deposits with pitting (photo b) and localized corrosion zones (photo c) confirmed by pitting profundity.

4. Conclusion

Results of this work indicate that for the protection of L80 stainless steel immersed in a multiphase medium, N-(2-aminoethyl) amine-based corrosion inhibitor has a satisfactory protective power and can be widely used, in particular because of its low toxicity towards environment. Indeed, for a dose of 50 ppm of this inhibitor, inhibiting efficiency obtained by polarisation resistance technique is 93%, and that measured by charge transfer resistance of EIS technique is 99.9%. Inhibitor addition to multiphase medium increased polarisation resistance of L80 steel, and slowed down its corrosion rate from $9.95.10^{-3}$ to

$7.11.10^{-5}$ mm/year for 0 to 50 ppm of inhibitor. Electrochemical Impedance Spectroscopy EIS results clearly show increase in capacitive loop diameter as inhibitor concentration increases, in line with the increase in polarization resistance.

Acknowledgments

Authors acknowledge collaboration with Research and Development Center Sonatrach-Boumerdes and laboratory of the National Company for Major Petroleum Works (ENGTP) Reghaia-Algeria.

Some results in this paper were presented at the 6th International Colloquium of corrosion and material's protection CMP'22 Which was held between 12 and 15 December 2022 in Hammamet, Tunisia (https://cmp22.corrosioncolloquium.com/).

References

[1] Sail, L.; Ghomari, F.; Khelidj, A.; Bezzar A.; Benali, O. La perte de masse dans l'inhibition de la corrosion d'un acier. *Lebanese Science Journal*, 14(1) : (2013) 87-106.

[2] Béranger G., Henry G., Sanz G. Le livre de l'acier. Technique et Documentation Lavoisier, 1994, p. 233.

[3] Haouame, H., Bensaada, Z., Etude gravimétrique de l'inhibition de corrosion de l'aluminium par l'huile essentielle de menthe verte (mentha spicata) en milieu salin (3.0% NaCl), Mémoire de Master en Génie des Procédés, université de Guelma (2022).

[4] Yahya T. Al-Janabi., An Overview of Corrosion in Oil and Gas Industry Upstream, Midstream, and Downstream Sectors, Chapter 1, Book Editor(s):Viswanathan S. Saji, Saviour A. Umoren, 14 February 2020.

[5] Chinedu I. Ossai, Brian Boswell, Ian J. Davies. Pipeline failures in corrosive environments-A conceptual analysis of trends and effects. Engineering Failure Analysis. Vol. 53, (2015), Pages 36-58.

[6]Rafael Amaya-Gómez, Mauricio Sánchez-Silva, Emilio Bastidas-Arteaga, Franck Schoefs, Felipe Muñoz. Reliability assessments of corroded pipelines based on internal pressure – A review. Engineering Failure Analysis. Vol.98, (2019), Pages 190-214.

[7] Tanane, O., Younes, A., El Bouari, A. Corrosion et protection de l'acier inoxydable 316L dans l'industrie. Editions Universitaires Européennes, ISBN. 363972223X, September 2017.

[8] H. Lahbib, S. ben Hassen, H. Gerengi, Y. ben Amor, Inhibition effect of Cynara cardunculus leaf extract on corrosion of St37 steel immersed in seawater with and without bleach solution, Chem. Eng. Commun. 208 (2021) 1260–1278. https://doi.org/10.1080/00986445.2020.1771320

[9] H. Lahbib, S. ben Hassen, H. Gerengi, M. Rizvi, Y. ben Amor, Corrosion inhibition performance of dwarf palm and Cynara cardunculus leaves extract for St37 steel in 15% H2SO4: a comparative study, J. Adhes. Sci. Technol. 35 (2021) 691–722. https://doi.org/10.1080/01694243.2020.1819701

[10] Oltra, R., Renaud, L., Dernoncourt, C. Erosion-corrosion studies of stainless steels: quantification of the erosion regime and the synergism between erosion and corrosion. Deuxième colloque européen, Corrosion dans les usines chimiques et parachimiques, 1994, Grenoble, vol. 2, pp 2-1 2-8.

[11] Amara Zenati, A. Étude du comportement des aciers API 5L X60 sollicités par contraintes mécaniques et milieu de sol Algérien Simulé. Thèse de doctorat, Faculté de technologie, Université Abou Bekr Belkaid–Tlemcen. ALGERIE (2014).126 p.

[12] Bendjebbour, A. Corrosion localisée des aciers API 5L-X52 de la ligne ASR/MP sollicite en sol algérien. Mémoire de magister, Faculté de

Technologie, Université Abou Bekr Belkaid– Tlemcen. ALGERIE (2011). 174 P.
[13] Benaksa Feyrouz. Etude de la corrosion aqueuse d'un acier inoxydable dans différents milieux. Master (2017). 76P. Université de Biskra. Algeria..
[14] Fédération française de l'acier 6 rue André Campra - 93212 La Plaine Saint-Denis CEDEX Fiche 14 - septembre 2013.
[15] Kouache, A., Khelifa, A., Hamitouche, H. Etude de l'efficacité inhibitrice d'un tensioactif cationique synthétise à partir d'une coupe pétrolière, dans la lutte contre la corrosion interne des pipelines. Séminaire national, « matériaux – corrosion »' SNMC2' Skikda – 27, 28 Novembre 2013, p14.
[16] Guerroudj, A. Synthèse et Etude de 1.2.4 Triazoles dérivés de l'Acide Stéarique Comme Inhibiteur de Corrosion. Master (2018). 79p. Université Dr. Tahar Molay, Saida-Algeria.
[17] Olfat E. Elazabawy, Omnia A.A. El-Shamy, Nour E.A. El-Sattar, Corrosion inhibitory characteristics, thermodynamics, and theoretical studies of N-((2-aminoethyl) carbamothioyl) acrylamide for carbon steel in 1 M HCl. Egyptian Journal of Petroleum. Vol. 32 (3), (2023), Pages 7-14.
[18] Attout, Z., Chehboune, L., Ouahbi, K,. Comparaison entre le comportement électrochimique d'un acier inoxydable L80 et d'un acier inoxydable aimanté dans un milieu multiphasique. Master (2019), Université M'hamed Bougara Boumerdes-Algeria.
[19] Bendaas Okba, Oukacha Cylia, Optimisation des paramètres de fonctionnement du déethaniseur (C701) et du débutaniseur (C-702) de la section de fractionnement du gaz à l'UTG de Guellala, Boumerdes- Algeria, 2017.
[20] Mennad, F. Etude de corrosion de l'acier API5CTGradN 80 dans des puits d'injection d'eau par l'inhibiteur N-(2-aminoéthyl). Mémoire de Master. Faculté des Hydrocarbure et des Energies renouvelable, Université Kasdi Merbeh-Ouargla, ALGERIE (2015). 32 p.
[21] M. Ko, B. Ingham, N. Laycock, D.E. Williams . In situ synchrotron X-ray diffraction study of the effect of microstructure and boundary-layer conditions on CO2 corrosion of pipeline steels. Corrosion Science. Vol. 90, (2015). Pages 192-201.
[22] Sarkari Khorrami, M., Ali Mostafaei, M., Pouraliakbar, H., Hossein Kokabi, A. Study on microstructure and mechanical characteristics of low-carbon steel and ferritic stainless steel joints. *Materials Science and Engineering: A.* 608(1): 2014, 35-45.
[23] David, G. Les aciers inoxydables. Propriété Mise en œuvre Emploi Normes. Technique et Documentation-Lavoisier 1990.
[24] Yuan-Chun Huang, Y.C. Lin, Jiao Deng, Ge Liu, Ming-Song Chen. Hot tensile deformation behaviors and constitutive model of 42CrMo steel. Materials & Design. Vol.53, (2014), Pages 349-356.
[25] L. Scoppio; M. Barteri; G. Cumino. Sulphide Stress Cracking Resistance of Supermartensitic Stainless Steel For Octg. Corrosion97, New Orleans, Louisiana, March 09 1997. NACE-97023.
[26] Ghemmit- Doulache Naima, Azzouni Bouchra, Meriouli Amina. Effect of marine biofilm on the electrochemical behaviorof stainless steel and titanium. Research Journal of Chemistry and Environment. Vol. 19 (3) March (2015). Pages 49-52.
[27] H Kherrab-Boukezzata, N Ghemmit-Doulache, M Bounoughaz, Slimane Boutarfaia. Electrochemical behavior of zinc anode in acidic zinc electrolyte - influence of lead as an impurity in zinc anodic dissolution. Journal of Fundamental and Applied Sciences 14 (2), 391-416.
[28] Gökmen Sığırcık, Tunç Tüken, Mehmet Erbil. Assessment of the inhibition efficiency of 3,4 diaminobenzonitrile against the corrosion of steel. Corrosion Science. Vol.102, (2016), Pages 437-445.
[29] Granese, S.L., Study of the Inhibitory Action of Nitrogen-Containing Compounds. Corrosion 44 (1998) 322-327.
[30] Bentiss, F., Lebrini, M., Traisnel, M., Lagrenée, M.Synergistic effect of iodide ions on inhibitive performance of 2,5-bis(4-methoxyphenyl)-1,3,4-thiadiazole during corrosion of mild steel in 0.5 M sulfuric acid solution. Journal of Applied Electrochemistry. 39, (2009) 1399–1407.
[31] Mohammed H. Othman Ahmed, Ahmed A. Al-Amiery, Yasmin K. Al-Majedy, Abdul Amir H. Kadhum, Abu Bakar Mohamad, Tayser Sumer Gaaz. Synthesis and characterization of a novel organic corrosion inhibitor for mild steel in 1 M hydrochloric acid. Results in Physics. Vol. 8, (2018), Pages 728-733.